

Article

Impact of Vineyard Inter-Row Management in Estimated Soil Erosion Under Actual and Future Rainfall Scenarios

Matteo Giganti ¹, Massimiliano Bordoni ^{1,*}, Antonio Gambarani ¹, Valerio Vivaldi ¹, Tommaso Frioni ², Alberto Vercesi ², Matteo Gatti ², Stefano Poni ² and Claudia Meisina ¹

¹ Department of Earth and Environmental Sciences, University of Pavia, Via Ferrata 1, 27100 Pavia, Italy; matteo.giganti@unipv.it (M.G.); antonio.gambarani01@universitadipavia.it (A.G.); valerio.vivaldi@unipv.it (V.V.); claudia.meisina@unipv.it (C.M.)

² Department of Sustainable Crop Production, Università Cattolica del Sacro Cuore, Via Emilia Parmense 84, 29122 Piacenza, Italy; tommaso.frioni@unicatt.it (T.F.); alberto.vercesi@unicatt.it (A.V.); matteo.gatti@unicatt.it (M.G.); stefano.poni@unicatt.it (S.P.)

* Correspondence: massimiliano.bordoni@unipv.it

Abstract

Sloping vineyards are highly susceptible to soil erosion driven by intense rainfall. Evaluating the impact of different soil management practices is crucial for implementing conservation strategies to mitigate this process. This study aims to estimate soil erosion under various inter-row management systems (permanent grass cover, alternating tillage, and different combinations of sown mixtures and termination methods) using a modeling procedure based on the Revised Universal Soil Loss Equation (RUSLE). The research was conducted in the Oltrepò Pavese (Northern Italy), a representative hilly vineyard area with medium steepness and clayey soils. Soil erosion was modeled at an annual scale, considering current conditions and three future climate projections (CMCC-CM2-VHR4, MPI-ESM1.2-XR, and EC-Earth3P-HR). Results indicate that annual soil loss is strongly influenced by inter-row management across all rainfall scenarios. Conservative practices—specifically cereal-based cover crops combined with rolling and sub-row mulching—significantly reduced erosion compared to alternating tillage, with average rates dropping from 1.85–3.30 Mg/ha/yr to 0.02–0.04 Mg/ha/yr. These findings underscore the importance of optimized interrow management in reducing soil degradation on sloping terrains.

Keywords: revised universal soil loss equation; sloping vineyards; inter-row managements; rolling; mulching



Academic Editor: Vito Ferro and Jeff Strock

Received: 27 February 2026

Revised: 11 May 2026

Accepted: 15 May 2026

Published: 18 May 2026

Copyright: © 2026 by the authors. Licensee MDPI, Basel, Switzerland. This article is an open access article distributed under the terms and conditions of the [Creative Commons Attribution \(CC BY\) license](https://creativecommons.org/licenses/by/4.0/).

1. Introduction

Soil is among the most valuable resources on the human timescale. Its fertility serves as the foundation for agricultural practices and plays an essential role in maintaining air and water quality, supplying 95% of our food, and ensuring climate stability [1]. However, this critical resource is continuously threatened by degradation processes, with soil erosion representing a primary cause [2].

Soil erosion is a natural geomorphic energy-driven process that involves the detachment, transport, and deposition of soil particles. The energy required for this process is supplied by various agents, which also define the type of erosional process. The four primary energy sources are physical forces (e.g., wind and water), gravity, chemical reactions, and anthropogenic disturbances such as tillage. Indeed, tillage implements constitute a

significant source of energy that can induce substantial downslope soil translocation. The intensity and rate at which energy is dissipated from these sources ultimately govern the severity of soil erosion [3]. Anthropogenic activities have dramatically accelerated the rate of soil erosion [4], leading to a global environmental challenge. When the rate of erosion surpasses the natural rate of soil formation (pedogenesis), it results in a net loss of this vital resource, triggering a cascade of negative on-site and off-site impacts, including loss of fertility and reduction of agricultural productivity [5]. The off-site impacts of soil erosion, such as sedimentation, flooding, landslides, and water eutrophication, impose costs borne by society at large rather than the individual landowner. During the 20th century, the increase in population has drastically accentuated the risks and extent of soil degradation [3].

Among the various erosive agents, water is a major driver of soil loss worldwide. Water erosion initiates when the soil is saturated and the rainfall intensity exceeds the soil's infiltration capacity, generating surface runoff [6]. The fight against this type of soil erosion is of particular urgency, as this phenomenon, with a global estimated annual loss of approximately 36 billion tons from inter-rill and rill processes alone, poses one of the most severe threats to global food security [7].

In European agricultural areas, where the mean soil loss rate is estimated at $4.21 \text{ Mg ha}^{-1} \text{ yr}^{-1}$ [8], permanent cropping systems such as vineyards, olive groves, and maize exhibit significantly higher erosion rates ($9.47 \text{ Mg ha}^{-1} \text{ yr}^{-1}$) compared to arable land ($2.67 \text{ Mg ha}^{-1} \text{ yr}^{-1}$) and pastures ($2.02 \text{ Mg ha}^{-1} \text{ yr}^{-1}$) [9].

In particular, the vineyard agroecosystem is one of the environments most threatened by soil erosion, commonly induced by rainfall, especially on sloping terrains [7,10], posing a severe threat to the long-term sustainability of local wine industries and of the sector in general. Besides the predisposing effect induced by hillslope morphology and soil physical features, a key strategy to mitigate soil erosion in these vulnerable agroecosystems is the establishment of ground covers between and under the rows [11,12]. The use of cover plants, like spontaneous vegetation or sown cover crops, or the application of mulch from pruning residues or straw, have been demonstrated as effective and sustainable measures to reduce the impact of severe rainfall events on soil detachment [13]. Moreover, homogeneous and mixed temporary cover crops enhance surface water infiltration and effectively reduce runoff compared to conventional tillage management [14].

The susceptibility of vineyards towards soil erosion induced by water could also rise as a consequence of climate change effects [15]. The increase in rainfall severity, especially for stronger events in tens of minutes and hours and the rise of cumulated rainfall amounts at seasonal or yearly scale [16], could induce the generation of more water runoff, provoking a higher rate of soil detachment at the hillslope scale [17]. This aspect determines how different soil management techniques in sloping vineyards could answer to significant rainfall amounts and to particular meteorological events induced by climate change [18].

Consequently, measuring soil erosion rates becomes crucial for understanding its spatial and temporal dynamics and for identifying effective mitigation strategies. The quantification of erosion-related processes in sloping vineyards can be performed by a range of methodological approaches proposed in the literature. Among these, the use of experimental plots in vineyard environments to directly measure sediment yield following rainfall events is a well-established practice [19]. Within this methodological framework, remote sensing techniques represent a robust and scalable means to investigate soil erosion dynamics. Recent advances in three-dimensional surveying technologies, coupled with innovative data processing and management strategies, have significantly expanded the analytical potential of geomorphological and hydrological studies in agricultural landscapes [20]. Light detection and ranging (LiDAR), implemented using unmanned aerial

vehicles (UAV), has emerged as a rapid, cost-effective alternative for high-resolution topographic surveying, allowing for retrieving digital elevation models (DEMs) with centimetric spatial resolution. This tool allows the detection and the digital representation of subtle micro-topographic features, creating datasets for the investigation of surface processes [21] with strong potential for erosion assessment and quantification [22]. Starting from these acquisitions, a commonly applied methodology for soil loss estimation involves the analysis of multi-temporal DEMs to derive DEMs of difference (DoD), which enable the spatial identification and quantification of erosion and deposition patterns [23]. Although this approach provides a detailed morphological characterization of surface change, it remains inherently descriptive, as it does not explicitly account for the governing processes responsible for erosion, such as rainfall erosivity, runoff generation, or sediment transport mechanisms [24]. Moreover, photogrammetry, based on structure of motion, permits the reconstruction of high-resolution 3D models of land surfaces, achieving centimetric accuracy on the detection of ground surface changes induced by soil erosion processes. [25–27].

Moreover, integrating multispectral and thermal sensors with UAV platforms allows for monitoring vegetation cover and soil moisture, critical factors in erosion processes [21]. Multispectral imagery, for example, can provide vegetation indices like NDVI, offering insights into plant health and erosion control [17,18].

Physically-based numerical models can represent a complementary approach capable of addressing these limitations, albeit at the expense of increased data requirements and computational complexity to explicitly simulate the underlying hydrological and sediment transport processes [28]. The Watershed Erosion Prediction Project (WEPP), for instance, requires detailed climatic, pedological, topographic, and land management inputs to simulate water balance components, soil detachment, sediment transport, and deposition at multiple spatial scales [29]. Moreover, the simulation of water erosion (SIMWE) model operates at the landscape scale to simulate overland flow, soil erosion, sediment transport, and deposition under spatially heterogeneous terrain, soil, vegetation cover, and rainfall excess conditions [30].

In this framework, the revised universal soil loss equation (RUSLE) is among the most widely implemented empirical models for predicting long-term average annual soil loss due to water erosion, integrating rainfall erosivity, soil erodibility, topographic factors, land cover, and conservation practices [31]. Nevertheless, the empirical nature and simplified structure of RUSLE impose well-documented constraints on its applicability, particularly under event-based erosion conditions [32,33]. By incorporating experimental calibration and field validation, RUSLE represents a well-established method for reconstructing long-term erosion rates at hillslope scales, providing yearly resolution while accounting for shifts in erosion rates induced by climate change [34–39].

Consequently, the application of soil erosion models such as RUSLE is essential for analyzing the impact of climate change on erosion trends within vineyard environments, particularly when considering how various soil management practices respond to these shifts. While numerous studies have already examined the effects of climate change on soil erosion patterns across different environmental and land-use contexts [6,7], few studies have estimated and analyzed soil erosion trends from current to projected future climatic conditions [34], while simultaneously accounting for the impact of different inter-row management strategies. In particular, refs. [12,40] identified a significant knowledge gap concerning the need for researches focused on assessing how different soil management, cover cropping, and intercropping systems affect erosion rates at various scales, from hillslopes to larger areas. To address this need, the present study aims to reconstruct soil erosion rate trends under both current and future climatic scenarios by implementing the RUSLE model across different vineyard soil management systems.

2. Study Area

2.1. Oltrepò Pavese Area

This work was carried out in a representative test-site of the Oltrepò Pavese region (northern Italy), a hilly wine-growing area of notable importance where soil erosion is a pressing issue.

Oltrepò Pavese (Figure 1) is a hilly-mountainous area of 1093 km², located in northern Italy and representing the northwestern termination of the Apennines. According to the last Italian ministry census, this is one of the most important and traditional Italian areas for wine production, with about 100,000 tons per year of wine [41].

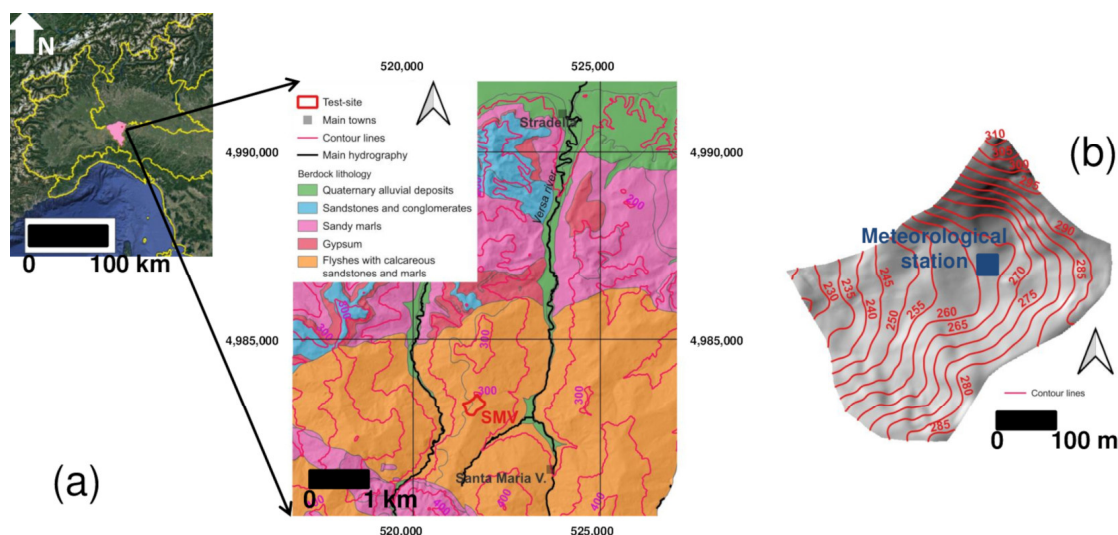


Figure 1. Location of the test site in Oltrepò Pavese area (a). Main topographical features of the test-site (b).

The altitude ranges between 60 and 1700 m above sea level (ASL), while the slope steepness ranges between 5 and 45°. According to Köppen's classification of world climates, the climatic regime of this zone is temperate/mesothermal, with a mean yearly temperature of 12 °C and a mean yearly rainfall amount of 737.6 mm (Canevino meteorological station, ARPA Lombardia monitoring network).

From the geological point of view, this area exhibits a complex geological structure characterized by the superimposition of Internal Ligurian Units over External Ligurian Units. In particular, in the northern sector, where the test sites are located, a Miocene-Pliocene sedimentary succession, consisting of poorly cemented conglomerates, sandstones, sandy marls and evaporitic formations (chalky marls and gypsum), are tectonically overimposed on eocenic flyshes composed predominantly of calcareous sandstone interbedded with marls [42,43].

The northern sector of Oltrepò Pavese is also characterized by a dense hydrographic network, dominated by the Versa River and its tributaries, with a seasonal hydrological regime typical of the northern Apennines, marked by high variability and rapid responses to rainfall events [40]. Research conducted in this area has demonstrated that intense precipitation can strongly influence runoff and sediment transport, underscoring the close interaction between topography, soil properties, and land use causing proneness of this territory to soil erosion [44].

The land use consists of a mosaic of agricultural and semi-natural systems, with vineyards forming the dominant element of the cultivated landscape (approximately 22%) [45].

Vineyards are typically cultivated on hilly settings with fine-textured soils, mainly with silty and clayey textures.

2.2. Test Site

An experimental test site (Figure 1b), labelled as SMV, was selected as representative of the main geological and geomorphological settings where vineyards are implanted in Oltrepò Pavese (Table 1). It had an area of 16.9 ha. It was characterized by medium slope steepness (range of slope angle between 0 and 27°), with a north-western to western aspect and altitude range of 220–310 m ASL. Soil was derived from a marly-arenaceous bedrock and presented typical thickness below 1 m and a clayey texture all along the study test site (Table 1). Soil permeability was in the range 10^{-6} – 10^{-5} m/s [41].

Table 1. Main geological and geomorphological features of the test-site.

Elevation (m ASL)	Slope Angle (°)	Slope Aspect	Bedrock Lithology	Sand (%)	Silt (%)	Clay (%)	Soil Thickness (m)	Soil Permeability (m/s)
257–287	0–27	NW-W	calcareous sandstones and marls	8	31	61	0.0–1.0	10^{-6} – 10^{-5}

The vineyards were characterized by the presence of different inter-row soil management (Table 2; Figure 2). Two traditional soil management approaches corresponded to a periodically mowed permanent grass cover (pgc) and to an alternating tillage between each inter-row (alt). In both the cases, the present grass species were spontaneous, with a typical mixture of grasses and ruderal broadleaf weeds common in vineyard inter-rows (e.g., *Lolium* spp., *Avena* spp., *Chenopodium* spp.). These managements have been carried out for at least the last 10 years.

Table 2. C factor for the land uses in the test site.

Land Use	Percentage in the Area (%)	Slope Angle Range (°)	Slope Angle Mean (°)	C Factor
wood land	6.1	6–27	15	0.001
field	17.7	0–27	13	1.000
dirt road	2.4	0–25	10	1.000
urban area/road	13.2	0–23	7	-
pgc vineyard	56.2	0–20	11	0.040
alt vineyard	3.0	6–25	14	0.350
gm_c	0.2	5–15	10	0.020
gm_n	0.5	5–15	10	0.060
r_c	0.2	5–14	11	0.050
r_n	0.3	5–15	11	0.600
sr_c	0.2	8–13	11	0.020
sr_n	0.1	6–9	8	0.060

Moreover, other soil management techniques were implemented, based on the sowing of two specific cover crop mixtures of different grass species (Table 2). A first one was a cereal-based mixture (_c) with the following seed composition: polystic barley (*Hordeum vulgare*), oats (*Avena strigosa*), crimson clover (*Trifolium incarnatum*), fodder rapeseed (*Brassica napus*), and blue tansy (*Phacelia tanacetifolia*). A second one was a leguminous plant-based

mixture (_n) with the following seed composition: common vetch (*Vicia sativa*), hairy vetch (*Vicia villosa*), and common oat (*Avena sativa*).

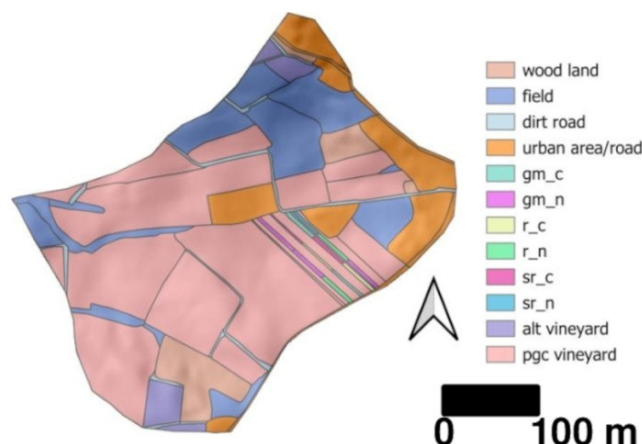


Figure 2. Land use map of the test site.

The two mixtures were sown in October, using a tractor mounting a pneumatic seeder combined with a power harrow, which allowed to reduce the size of clumps eventually formed during seedbed preparation. Cover crops grew during autumn and winter months until the complete and mature stages in spring. After the half of May, the two mixtures were terminated with three different types of managements [46]: (i) rolling (r_) performed by mechanically compressing the cover crop at its maximum growth; (ii) sub-row mulching (sr_), consisting of mechanically slashing and piling under the row the resulting biomass to form an organic and dead mulch layer; and (iii) green manure (gm_), consisting of mechanically cutting the biomass, which were then incorporated into the soil forming a below ground level at around 0.2–0.3 m from the surface. The combination of termination methods and sown species resulted in 6 treatments: r_c, sr_c, gm_c, r_n, sr_n, and gm_n. These six treatments were kept steady between June and September, after a new sowing the next October. These treatments were implemented in the period 2021–2025.

Other land uses were present in the test site, corresponding to: urban areas and roads; dirt roads; fields considered as fallow for most of the year, due to the absence of a continuous agronomical management and grass cover; and wood lands of broadleaves species, mainly composed of *Robinia pseudoacacia* (Figure 2).

The percentage of the area occupied by each land use was very different (Table 2). However, the comparison between the impact of soil managements on soil loss in vineyards was possible, since the range (0–20°) and the mean values (8–14°) of slope angle were similar between the vineyards with different interrow management.

3. Materials and Methods

3.1. Analysis of the Rainfall Trends

A meteorological station (MeteoSense 4.0, Netsens s.r.l., Calenzano, Italy) was installed in the test site for the acquisition of the main meteorological variables: rainfall amount, air temperature and humidity, atmospheric pressure, wind speed, and total solar radiation. Daily rainfall amounts were retrieved from this station for the years 2021–2025. These data were, then, merged to daily rainfall amounts acquired by the closest rain gauge of the Arpa Lombardia monitoring network (Canevino meteorological station, 7 km away from the test site) for 2004–2020 time span. Daily amounts of each year were summed to obtain the yearly cumulated amounts, for covering the period between 2004 and 2025.

The actual rainfall trends were coupled with three future scenarios of yearly rainfall amounts covering the period 2026–2050, obtained from daily future trends of rainfall derived from the three following models: (i) the CMCC-CM2-VHR4 climate model (for more details on model building and main principles we refer to [47]); (ii) the MPI-ESM1.2-XR climate model (for more details on model building and main principles we refer to [48]); and (iii) the EC-Earth3P-HR in PRIMAVERA climate model (for more details on model building and main principles we refer to [49]). These data were retrieved from the open-source weather API called Open-Meteo (<https://open-meteo.com/>; accessed on 7 January 2026).

The future scenarios of rainfalls were calculated for 4 cells around the test sites, obtaining an average trend for each of the adopted model. The innovative trend analysis (ITA) was, then, calculated for a general indication of rainfall trend on the test site between actual and future scenarios [50]. In particular, the yearly time series of actual and of each future scenarios were sorted in ascending order. The two obtained sub-series were plotted on x-axis and y-axis of a Cartesian plane, classifying in three magnitude ranges (low, medium, and high). If the data lie along the 1:1 (45°) line, no trend is present in the time series. When sample points are concentrated in the upper triangular region above the 45° line, the time series exhibits an increasing trend; conversely, a decreasing trend is observed when the points fall in the lower triangular region below the line. Since this method can be applied to time series of the same length, future scenarios in the time span between 2026 and 2047 were considered to have the same length (21 years) of the actual time series (2004–2025).

3.2. Application of the RUSLE Model

Figure 3 shows the flowchart of application of the RUSLE model in a distributed approach across the test site, carried out through QGIS software (version 3.38; <https://qgis.org/>). The RUSLE model has been developed for the estimation of the average annual soil loss induced by rainfall erosive forces [31]. According to this, RUSLE model is based on an equation (Equation (1)) that is able to estimate the soil loss at yearly scale (A ; measured in $\text{Mg ha}^{-1} \text{ year}^{-1}$) by a set of factors influencing erosion dynamics:

$$A = R \times K \times LS \times C \times P \quad (1)$$

where R is the rainfall-runoff erosivity factor ($\text{MJ mm ha}^{-1} \text{ h}^{-1} \text{ year}^{-1}$), K is the soil erodibility factor ($\text{Mg ha h ha}^{-1} \text{ MJ}^{-1} \text{ mm}^{-1}$), LS is the slope length and steepness factor (dimensionless), C is the cover-management factor (dimensionless), and P is the support practice factor (dimensionless). The detailed description of the method is reported in [31].

According to this equation, RUSLE model could be applied considering yearly rainfall data, allowing to the estimation of yearly soil loss [6].

Within the RUSLE model, the rainfall erosivity R is a critical parameter, as precipitation is the primary driver of soil erosion [51]. At a yearly timescale, this factor represented the average of the kinetic energy and intensity of rainfall, quantifying its capacity to cause sheet and rill erosion. It is calculated from the kinetic energy of individual storms, aggregated over a year. For the R factor, the site being small, the factor remains steady within the test site. With the same amount of rainfall, the main difference in erosion for the same type of management must be other factors. The estimation of R was, then, obtained by Equation (2), which could be applied, considering the mean cumulative-daily precipitation over a particular year or along a longer time series, taking into account a deterministic procedure for the assessment of the erosivity factor [52]:

$$R = \frac{\left(\sum_1^n \sum_1^{365} \left(0.11 P_{day}^{1.82} \right) \right)}{n} \tag{2}$$

where 0.11 is a constant, Pday is the mean daily rainfall, and n is the number of years.

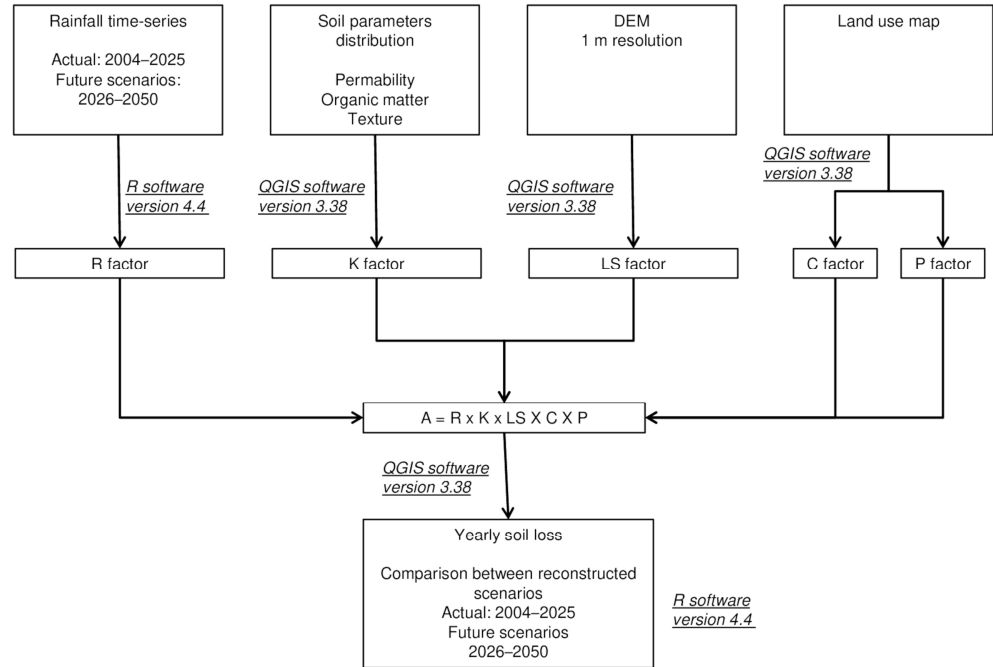


Figure 3. Flowchart of the application of RUSLE model in the test site.

Regarding the K-factor, it reflects soil susceptibility to erosion as influenced by texture, organic matter content, structure, and permeability [53]. Soil erodibility was calculated using Equation (3) [54]:

$$K = \frac{[2.77 \cdot 10^{-7} (12 - OM) M^{1.14} + 4.28 \cdot 10^{-3} (s - 2) + 3.29 \cdot 10^{-3} (p - 3)]}{100} \tag{3}$$

where M is the textural factor, calculated based on the particle-size fractions (fine material and coarse material equal to 33 and 6% of the soil texture, respectively; clay amount equal to 61%) as specified in Table 1; OM is the organic matter content percentage (fixed at 2.4% for this study, calculated as the average of four measurements from soil samples taken at the test site within the top 0.3 m of soil); s represents the soil structure code, which ranges from 1 to 4; a value of 1 was assigned to the test site based on its very fine granular structure; and p is the permeability class code, ranging from 1 to 6 based on saturated hydraulic conductivity. A value of 3 was assigned to p, corresponding to moderate permeability given the measured range of 10⁻⁵ to 10⁻⁶ m/s obtained through Amoozometer measures and converted for p estimation through the method in [55]. Due to the homogeneous soil characteristics across the test site, the K-factor remained constant at 0.001 Mg·h·(MJ·mm)⁻¹·ha⁻¹ throughout the study area.

The LS factor, representing slope length and steepness, was calculated following the approach proposed by [56,57]. The calculation was performed using a 1 m resolution DEM of the study area, derived from LiDAR data acquired between 2008 and 2010 by the Italian Ministry for Environment, Land, and Sea, as part of the Extraordinary Plan of Environmental Remote Sensing (PST-A). Specifically, the LS factor was determined using Equation (4):

$$LS = \left(\frac{A_s}{22.13} \right)^m \times \left(\frac{\sin\beta}{0.0896} \right)^n \quad (4)$$

where A_s is the specific catchment area (up to 144 m in the test-site), that corresponds to the ratio of the upstream catchment area of a contour line to its length [58]; β is the slope angle in the test site (ranging between 0 and 27°); and m and n are equal to 0.4 and 1.3, respectively. LS was calculated according to the original DEM resolution at 1 m, while its values ranged between 0 and 92.822 (Figure S1 in Supplementary Material).

The C factor represented the impact of vegetation and crops in the reduction of soil erosion. The denser was the vegetation, and the lower could be the loss of soil. C factor was estimated for each land use and soil management in the vineyards inter-rows present in the test site (Table 2), according to reference values of the main plant species present in each land cover [6,59–61]. The values of C factor were obtained to the literature referred to sloping terrains, in particular those located in European environments, where rainfall and air temperature statistics are in range similar to the selected test site.

The P factor considered erosion control measure practices to reduce runoff velocity and sediment delivery. It was defined as the ratio between soil loss under a given soil conservation practice and the soil loss observed in a field managed with upslope and downslope tillage [31]. In this study, because no support practices were implemented in the test site, the P factor was set equal to 1 [17].

Table 3 lists the values of the different factors in the test site, while Figure S1 in Supplementary Materials provided the map of distribution of K , LS , and C factors in the test site.

Table 3. Values of the factors for the implementation of the implementation of the RUSLE model.

RUSLE Factor	Value
R	Different scenarios according to actual climatic conditions (2004–2025) and future forecasted climatic conditions (2026–2050). Future forecasted climatic scenarios are available at the open-source weather API called Open-Meteo (https://open-meteo.com/ ; accessed on 7 January 2026)
K	0.001 Mg·h·(MJ·mm) ^{−1} ·ha ^{−1} (moderate permeability class) Distributed across the test site, according to morphological features and distribution of slope length and steepness in the area. The calculation was performed using a 1 m resolution DEM, derived from LiDAR data acquired between 2008 and 2010 by the Italian Ministry for Environment, Land, and Sea, as part of the Extraordinary Plan of Environmental Remote Sensing (PST-A)
LS	Distributed across the test site, according to land use distribution in the area (Figure 2). The original land use distribution was converted in a distributed map of C factor, according to the values in Table 2 and using the same 1 m resolution for DEM and DEM-derived factors
C	

Since the availability of different rainfall scenarios, RUSLE was calculated modifying R factor in order to consider the impact of changes in yearly rainfall amounts. First, RUSLE was applied to estimate the average yearly soil loss in the actual rainfall scenario, corresponding to 2004–2025 time span. Then, RUSLE was applied to estimate the average yearly soil loss for all the three considered future rainfall scenarios in 2026–2050 time span. These analyses allowed to evaluate how the amount of yearly soil loss could change in

future respect to actual rainy conditions, focusing also on differences on soil loss between the different soil managements.

The erosion rates estimated by RUSLE for the actual scenario were validated by field measures in the vineyards with the different managements present in the test site. The stock unearthing measurement (SUM) [62,63] method was used to assess soil erosion, based on the assumption that the vertical distance between the graft union and the original soil surface could change over time for processes causing soil loss. These measures consisted in a manual measurements with a ruler of the distance between the graft union and the soil surface in a particular time. The difference of the original graft union height with respect to this measure depended on the soil loss over this time span. In the test site, an initial graft union height of 15 cm was adopted. Moreover, the dry weight of the soil, required to convert the measures from distances to soil loss, was equal to 10.6 Mg/m^3 . The age of the vineyards, required for calculating the average soil loss, was equal to 20 years. According to [62], the accuracy of the SUM method is equal to 0.5 cm, corresponding in the test site to a value of 0.009 Mg/ha/year . The measurements were carried out in 34 locations with different managements of the vineyards throughout the study area.

3.3. Statistical Analyses

Statistical analyses were conducted to assess similarities and differences in average total yearly soil loss estimated by RUSLE for the different land uses in each scenario. This analysis allowed to evaluate statistically which land uses could induce the same erosion pattern in the test site.

Normality on the distribution of the soil loss values was assessed using the Shapiro–Wilk test. Since p -values were lower than 0.001, data were not normally distributed. Thus, a non-parametric test was used to compare the soil loss values in different land uses, using also the climatic scenario as covariate factor. In particular, the Scheirer–Ray–Hare test was used, taking into account the rainfall scenario and the land uses as fixed effects and the average total yearly soil loss as random effect. In addition, the significance of the interaction between fixed effects and the associated random effect was evaluated, following the recommendations of [64].

When significant differences among the soil loss in different classes of the factors were detected, the Dunn's test was applied for post hoc multiple comparisons.

All these tests were verified for p -values of 0.05. These statistical analyses were applied through R software (version 4.4; <https://www.r-project.org/>).

4. Results

4.1. Rainfall Trends

Yearly rainfall amounts in actual and future climatic conditions have been analyzed for identifying possible changes along time. Average yearly rainfall amount for the period 2004–2025 was equal to 737.6 mm, with a minimum value of 390.6 mm and a maximum amount of 1140.6 mm. The three considered future scenarios for the period 2026–2050 estimated higher yearly cumulated rainfalls, since the mean values were of 1073.4, 1085.6, and 1129.2 mm for CMCC-CM2-VHR4, MPI-ESM1.2-XR, and EC-Earth3P-HR, respectively. ITA test on yearly cumulated amounts confirmed the rise of this attribute for all the future forecasted scenarios, with an evident positive trend (Figure 4). In particular, the increase on yearly rainfall amount was estimated of 45.5, 47.2, and 53.1% than the actual climatic condition for CMCC-CM2-VHR4, MPI-ESM1.2-XR, EC-Earth3P-HR, respectively.

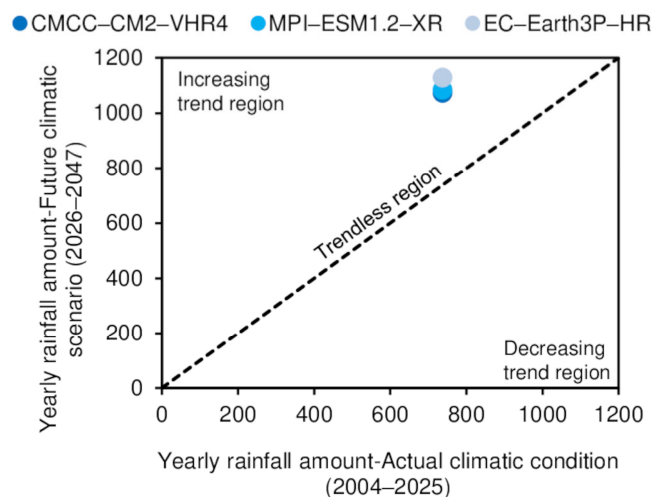


Figure 4. Results of the ITA test applied to the series of yearly rainfall amount at the test site.

4.2. *RUSLE Modeling for Actual and Future Climatic Conditions*

The application of RUSLE model allowed to identify the soil erosion pattern in the test site for actual and future climatic scenarios. The application of Scheirer–Ray–Hare test demonstrated statistically significant differences between estimated soil loss in different land uses ($H_{10,208} = 222.89$, p -value > 0.001), regardless of the considered climatic scenario ($H_{3,208} = 2.88$, p -value = 0.41) and without any interaction between these two covariates ($H_{30,208} = 7.49$, p -value = 0.99). A post-hoc Dunn’s test (Table S1 in Supplementary Material) showed that the pairs with field, dirt road, and wood land classes were characterized by values of the total soil loss significantly different within the classes of the pairs.

Figure S2 in Supplementary Material and Table 4 show the results of RUSLE application according to actual climatic conditions in 2004–2025 time span. Due to the higher C-factor values, fields and dirt roads were characterized by the highest amounts of yearly soil loss, averagely overpassing 9 Mg/ha/yr. Instead, estimated soil loss in vineyards was lower, since it kept averagely below 2 Mg/ha/yr. However, vineyards with alternating tillage showed a higher soil loss than the other managements, where average soil loss was below 1 Mg/ha/yr. Moreover, the soil managements derived by the termination of sown mixture based on cereals (gm_c, r_c, sr_c) had the lowest soil loss than the other implemented managements of vineyards inter-rows, with average values in the range of 0.02–0.10 Mg/ha/yr.

Table 4. Range of the soil loss estimated by RUSLE according to actual climatic conditions in the test-site.

Land Use	RUSLE Soil Loss for Actual Climatic Conditions (2004–2025) (Mg/ha/yr)
wood land	0.003–0.10
field	5.00–37.00
dirt road	6.00–95.51
urban area/road	-
pgc vineyard	0.10–0.40
alt vineyard	0.02–2.00
gm_c	0.10–2.00
gm_n	0.20–3.00
r_c	0.002–0.05
r_n	0.30–2.00
sr_c	0.02–0.03
sr_n	0.60–3.00

The modeled values estimated with RUSLE model for the actual scenario were validated by the field measures of the SUM method in the differently managed vineyards. The field measures confirms the trends on erosion rates observed with RUSLE modeling, besides differences of 0.01–1.03 Mg/ha/yr on average between field and RUSLE estimations (Table 5). As already shown by RUSLE modeling, alt vineyard was, again, the most susceptible management, with soil loss of 0.83 Mg/ha/yr on average. The other vineyard managements had field values of soil loss significantly lower, ranging between 0.15 and 0.22 Mg/ha/yr on average.

Table 5. Comparison between the average soil loss estimated by RUSLE according to actual climatic conditions and the field measures through SUM method for the different types of vineyards in the test-site.

Land Use	RUSLE Soil Loss for Actual Climatic Conditions (2004–2025) (Mg/ha/yr)	Field Measures of Soil Loss by SUM Method (Mg/ha/yr)
pgc vineyard	0.21	0.20
alt vineyard	1.85	0.83
gm_c	0.10	0.18
gm_n	0.33	0.19
r_c	0.02	0.15
r_n	0.25	0.21
sr_c	0.03	0.19
sr_n	0.33	0.22

Similar trends could be highlighted also in the considered future climatic scenarios (Figures 5 and 6). A general increase in soil loss in the land uses characterized all the future climatic scenarios, according to the rise in yearly rainfall amounts than the actual conditions. In particular, the increase in soil loss is in the order of 40.5, 50.2, and 77.9% for CMCC-CM2-VHR4, EC-Earth3P-HR, and MPI-ESM1.2-XR, respectively. Since the rise in soil loss was similar in percentage within each climatic scenario, field and dirt roads had, again, the highest average yearly soil loss, reaching up to 16.4 and 25.8 Mg/ha/yr in MPI-ESM1.2-XR, respectively.

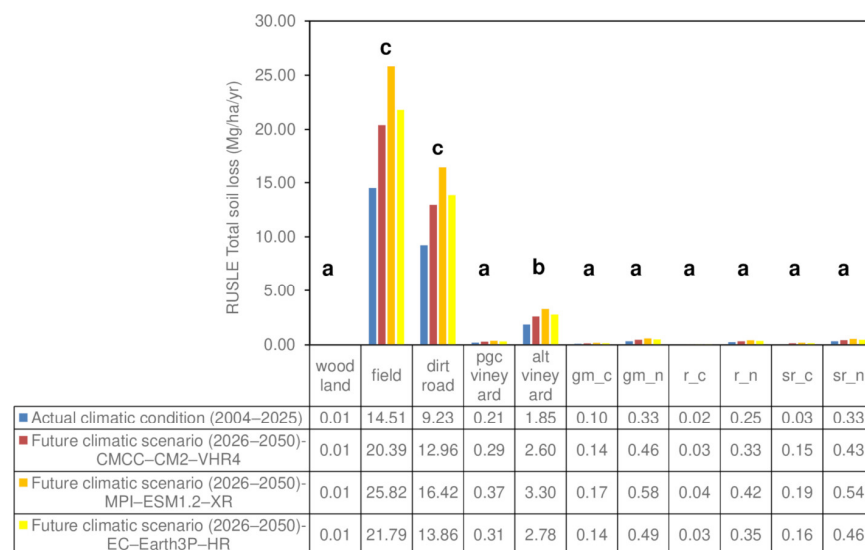


Figure 5. Soil loss estimated by RUSLE for all the land uses of the test site, for all the considered climatic scenarios. Different letters mean significant differences in the climatic conditions according to the Dunn test $p < 0.05$.

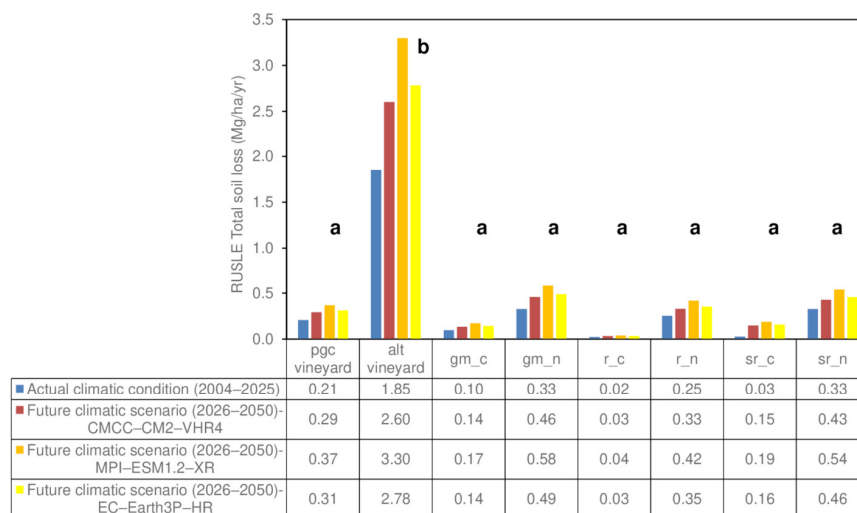


Figure 6. Soil loss estimated by RUSLE for the different vineyards managements in the test site, for all the considered climatic scenarios. Different letters mean significant differences in the climatic conditions according to the Dunn test $p < 0.05$.

The same increase affected also the different tested vineyards managements. Alternating vineyards (alt vineyards) were characterized again by the highest average yearly soil loss, reaching mean values between 2.6 and 3.3 Mg/ha/yr. Vineyards with permanent grass cover in the inter-rows (pgc vineyards), r_n, sr_n, and gm_n had soil loss in the range 0.3–0.6 Mg/ha/yr on average, while gm_c, r_c, and sr_c presented the lowest values of soil loss on average, with values below 0.2 Mg/ha/yr.

5. Discussion

The selected test site is representative of one of Northern Italy’s most traditional and premier wine-growing regions. It is characterized by clay-rich soil, moderate permeability, and medium slope steepness across the entire area. Consequently, the primary variations in erosion patterns are driven by land-use types and their distribution. Furthermore, a clear increase in erosion susceptibility was observed when transitioning from current to projected climatic conditions through 2050, regardless of the land-use type. This increasing trend was in agreement with other local and regional analyses all over the world [65,66], which highlighted an estimated and clear rise in yearly total soil loss due to a forecasted growth in yearly rainfall erosive force induced by climate change [67–70]. The three considered future climatic scenarios (CMCC-CM2-VHR4, EC-Earth3P-HR, and MPI-ESM1.2-XR) determined an average increase in yearly rainfall amounts at the test site between 45.5 and 53.1%, accounting for an estimated average growth of total soil loss of 40.5, 50.2, and 77.9% for CMCC-CM2-VHR4, EC-Earth3P-HR, and MPI-ESM1.2-XR, respectively.

Despite the most vulnerable land uses to soil erosion at test site were fields and dirt roads, the results of RUSLE modeling in different climatic scenarios gave significant outcomes on the relative effectiveness of the different management practices in vineyards to soil erosion proneness. This aspect was also demonstrated by the results of the Scheirer–Ray–Hare test, which showed a statistically significant difference between estimated soil loss in different land uses ($H_{10,208} = 222.89$, p -value > 0.001), regardless of the considered climatic scenario ($H_{3,208} = 2.88$, p -value = 0.41).

All the tested management techniques in soil inter-row of vineyards were at least 5–8 times less vulnerable to soil erosion than fallow open fields (fields) and dirt roads on average. However, the differences on estimated total soil loss between different inter-row management techniques was evident. Vineyards with alternated tillage in the inter-row (alt

vineyards) were consistently the most vulnerable treatment to soil erosion, with average yearly soil loss of 1.85 Mg/ha/yr and of 2.60–3.30 Mg/ha/yr in current and future climatic trends, respectively. In the hierarchy of the different vineyard soil management approaches, sowing leguminous-based cover crops (gm_n, r_n, sr_n) had yearly erosion rates 5 times lower than the ones of alternated tillage vineyards. Inter-rows with permanent spontaneous grass cover showed yearly erosion rates 9 times lower than the ones of vineyards with alternated tillage. Sowing cereal-based mixtures (gm_c, r_c, sr_c) allowed yearly erosion rates ranging 19–87 times lower than the ones of vineyards with alternated tillage. The r_c soil management, characterized by the mechanical rolling of the sown cereal-dominated cover crop biomass, had the lowest soil loss amounts, 0.02–0.04 Mg/ha/yr on average.

According to the tolerable limits of soil erosion, typically in the range between 2 and 12 Mg ha⁻¹ yr⁻¹ for environmental contexts similar to the test site [71–75], only alt vineyards in the test site were characterized by yearly soil loss close or slightly over these tolerance thresholds, since they had average values of soil loss between 1.85 and 3.30 Mg/ha/yr. Instead, the other vineyard managements presented a tolerable level of yearly soil erosion, since their values were below the limit of 2 Mg/ha/yr, both for actual and future climatic scenarios.

First, these results confirmed the negative effect of tillage operations in sloping soils, since, according to RUSLE, vineyards with alternating tillage were significantly more prone to soil loss than other less invasive managements. In fact, seasonal tillage showed to make the soil more vulnerable to particle detachment induced by rainfall events [76,77].

More conservative practices, such as permanent grass cover with spontaneous species or green manure and rolling and sub-row mulching from sown mixtures, were more effective in soil conservation, thanks especially to the lowest amounts of agronomical operations that could impact the structure of the soil [10]. However, the performance of mixtures with different compositions, in terms of soil protection against soil erosion, was not equal. In fact, the cereal-based mixture proved to be more resilient against erosion than the spontaneous natural and the leguminous-based mixtures.

The reason may be related to the different root system architectures characterizing these plant species. Cereal crops are characterized by a fibrous root system, with a high root density in the upper 10–20 cm of soil and roots that also develop laterally from the stem, allowing greater root reinforcement in the superficial soil horizons and enhanced aggregation of soil particles [78]. In contrast, mixtures dominated by legumes or by spontaneous species with mixed legume–cereal composition tend to exhibit a taproot system, with a thicker central root penetrating deeper into the soil and few lateral roots. As a result, these systems occupy less soil volume in the upper horizons and provide lower root reinforcement in the superficial soil layers [79].

However, for the same mixture, the chosen termination, predominantly made in late spring, could affect soil susceptibility to erosion. Green manure, which involves the incorporation of the cut biomass into the soil, is a technique that requires soil disturbance operations, potentially disrupting root systems and the soil structure itself. This may lead to a decrease in the C factor, thereby enhancing soil proneness to erosion, particularly during the summer and autumn months [80,81]. In contrast, rolling and sub-row mulching techniques do not involve soil disturbance, allowing greater soil cohesion and aggregate stability to be maintained and consequently reducing the soil predisposition to erosion [11].

These outcomes suggest that the selection of appropriate soil management in the inter-row is critical for mitigating rainfall-induced erosion in sloping vineyards. Temporary or continuous cover crops, possibly terminated with more conservative operations, could allow to reduce the impact of rainfall erosive forces, decreasing the rate of yearly soil loss.

Moreover, a cereal-based cover crop, or a mixture containing a significant proportion of cereals, may offer the optimal combination to enhance soil protection.

6. Limitations and Future Opportunities

Besides the achieved results, some limitations and future developments for this work could be underlined.

Soil loss was estimated on an annual scale by incorporating daily rainfall amounts into the calculation of the RUSLE R factor. However, since the greatest proportion of erosive events is often concentrated during short-term (e.g., hourly) intense rainfall [82], this approach may underrepresent peak erosivity. Consequently, soil loss assessments—under both current and future climatic scenarios—could be significantly refined by integrating hourly or sub-hourly rainfall intensity into the R factor estimation. This would better account for the impact of high-intensity, short-duration events, which are projected to intensify due to climate change in the Mediterranean basin [83–85]. Furthermore, annual erosion assessments could be coupled with event-based monitoring and modeling. This multi-scale approach could involve the repeated acquisition of high-resolution (centimetric) DEMs via UAV techniques [24], the implementation of sediment traps at various hillslope positions [86,87], rainfall simulator experiments [77], and the application of physically based soil erosion models [88].

The comparison between the impact of different land uses on soil erosion were performed in a small test site (16.9 ha), where slope steepness was medium-high, with typical values for vineyards up to 15°. Moreover, the percentage of the area in the test site occupied by the innovative techniques (gm_n, r_n, sr_n, gm_c, r_c, sr_c) was significantly lower than the ones covered with vineyards with the most traditional approach. The obtained results should be verified and got stronger by applying similar modeling approaches in other environmental settings in Italy and in Mediterranean areas, considering soils with different properties, larger test sites, and bigger areas, especially those occupied by sown mixtures also in correspondence of steeper hillslopes.

Since the positive impacts assessed for soil management approaches were based on rolling and sub-row mulching, a comprehensive assessment of the effects of these practices to the plants and their performances, both in terms of yield and grape quality, should be performed [11]. This aspect becomes fundamental in order to find vineyard managements able to counteract soil erosion, guaranteeing also a positive agronomic performance and economic sustainability for grapevine cultivation.

7. Conclusions

This work contributes to the analysis of the effects of different management of vineyard inter-rows on soil erosion susceptibility, considering a test site representative of the traditional viticultural areas of Northern Italian Apennines. Estimated yearly soil loss, by the application of RUSLE according to rainfall scenarios of actual and projected future climatic conditions, is strongly influenced by the management of the inter-row soil. Alternating tillage between rows promotes erosion, compared to other conservative practices limiting the tillage operations and maintaining spontaneous grassing or sowing cereal-based or leguminous-based mixtures. These approaches could allow to significantly reduce soil loss, especially for hillslopes with medium steepness and clayey soils.

The response of the most conservative approaches to soil erosion depend also on the composition of the plant mixture and the type of termination, carried out generally at the end of spring. Cereal-based mixture could decrease yearly soil loss, thanks to their peculiar root apparatus, which is able to reinforce more soil strength and aggregation. Furthermore, rolling and sub-row mulching of that mixture could reduce soil erosion susceptibility than

green manure, due to the maintenance of the cover crop also during summer and autumn months. These practices could allow to keep low values of yearly soil loss also in future projected climatic scenarios, when rainfall amounts up to 2050 could increase significantly at the test site.

The achieved results highlight the importance of implementing the best management in vineyard inter-rows to reduce the amount of soil loss in sloping terrains, also underlying the different responses of sown or spontaneous grass cover and of the termination operations. However, further works are required to verify the impact on soil erosion proneness for the same managements, considering different settings of slope steepness and soil type and also taking into account the agronomical performances of the grapevines, avoiding negative impacts for yields and grape quality. Moreover, more detailed quantification and estimation of soil erosion are required for assessing the impacts of daily and sub-daily concentrated and intense rainfall events in correspondence of different soil managements.

Supplementary Materials: The following supporting information can be downloaded at: <https://www.mdpi.com/article/10.3390/w18101217/s1>, Figure S1: Maps of distribution of K, LS and C factors in the test-site; Figure S2: Soil loss (in Mg/ha·year) estimated by RUSLE model for actual climatic conditions (2004–2025 time span); Table S1: Results of post-hoc Dunn’s test. Pairs which are statistically similar (confidence level with *p*-value of 0.01) are in bold characters.

Author Contributions: Conceptualization, M.G. (Matteo Giganti) and M.B.; methodology, M.G. (Matteo Giganti); software, M.G. (Matteo Giganti); validation, M.G. (Matteo Giganti), A.G., V.V. and T.F.; formal analysis, M.G. (Matteo Giganti); investigation, M.G. (Matteo Giganti); resources, M.G. (Matteo Giganti), M.B. and T.F.; data curation, M.G. (Matteo Giganti); writing—original draft preparation, M.G. (Matteo Giganti); writing—review and editing, M.B., A.G., V.V., T.F., A.V., M.G. (Matteo Gatti), S.P. and C.M.; visualization, M.G. (Matteo Giganti) and M.B.; supervision, M.B. and C.M.; project administration, M.B. and T.F.; funding acquisition, M.B. and T.F. All authors have read and agreed to the published version of the manuscript.

Funding: This research was in the frame of the project “New approaches to soil management for the improvement of vineyard resilience to climate change pressures (UNDER-VINE)”, grant number 20229E8S9A, funded by the European Union—NextGenerationEU—NRRP Mission 4, Component 2, Investment 1.1 ‘Fund for the National Research Programme and Projects of National Interest (NRP)’, MUR Directorial Decree 104 of 2 February 2022 (Notice PRIN 2022).

Data Availability Statement: The raw data supporting the conclusions of this article will be made available by the authors on request.

Acknowledgments: The authors sincerely thank Enrico Ottina for kindly making its vineyard available for this work activities. We also thank the Academic Editor and the Anonymous Reviewers for their comments and suggestions.

Conflicts of Interest: The authors declare no conflicts of interest.

Abbreviations

The following abbreviations are used in this manuscript:

LiDAR	Light Detection and Ranging
UAV	Unmanned aerial vehicles
DEM	Digital Elevation Model
DoD	DEMs of Difference
WEPP	Watershed Erosion Prediction Project
SIMWE	Simulation of Water Erosion
RUSLE	Revised Universal Soil Loss Equation
pgc	Periodically mowed permanent grass cover
alt	Alternating tillage between each interrow

_n	Leguminous plants-based mixture
_c	Cereal-based mixture
r_	Rolling
sr_	Sub-row mulching
gm_	Green manure
ITA	Innovative Trend Analysis

References

1. FAO. *The State of Food and Agriculture 2023—Revealing the True Cost of Food to Transform Agrifood Systems*; FAO: Rome, Italy, 2023. [\[CrossRef\]](#)
2. Oishy, M.N.; Shemonty, N.A.; Fatema, S.I.; Mahbub, S.; Mim, E.L.; Raisa, M.B.H.; Anik, A.H. Unravelling the effects of climate change on the soil-plant-atmosphere interactions: A critical review. *Soil Environ. Health* **2025**, *3*, 100130. [\[CrossRef\]](#)
3. Lal, R. Soil degradation by erosion. *Land Degrad. Dev.* **2001**, *12*, 519–539. [\[CrossRef\]](#)
4. Lopez-Vicente, M.; Calvo-Seas, E.; Álvarez, S.; Cerdà, A. Effectiveness of cover crops to reduce loss of soil organic matter in a rainfed vineyard. *Land* **2020**, *9*, 230. [\[CrossRef\]](#)
5. Panagos, P.; Vieira, D.; Eekhout, J.P.C.; Biddoccu, M.; Cerdà, A.; Evans, D.L.; Tavoularis, N.; Bezak, N.; Negrel, P.; Katsoyiannis, A.; et al. How the EU Soil Observatory contributes to a stronger soil erosion community. *Environ. Res.* **2024**, *248*, 118319. [\[CrossRef\]](#)
6. Panagos, P.; Borrelli, P.; Poesen, J.; Ballabio, C.; Lugato, E.; Meusburger, K.; Montanarella, L.; Alewell, C. The new assessment of soil loss by water erosion in Europe. *Environ. Sci. Policy* **2015**, *54*, 438–447. [\[CrossRef\]](#)
7. Borrelli, P.; Robinson, D.A.; Fleischer, L.R.; Lugato, E.; Ballabio, C.; Alewell, C.; Meusburger, K.; Modugno, S.; Schütt, B.; Ferro, V.; et al. An assessment of the global impact of 21st century land use change on soil erosion. *Nat. Commun.* **2017**, *8*, 2013. [\[CrossRef\]](#)
8. Keesstra, S.D.; Bouma, J.; Wallinga, J.; Tiftonell, P.; Smith, P.; Cerdà, A.; Montanarella, L.; Quinton, J.N.; Pachepsky, Y.; van der Putten, W.H.; et al. The significance of soils and soil science towards realization of the United Nations Sustainable Development Goals. *SOIL* **2016**, *2*, 111–128. [\[CrossRef\]](#)
9. Novara, A.; Stallone, G.; Cerdà, A.; Gristina, L. The effect of shallow tillage on soil erosion in a semi-arid vineyard. *Agronomy* **2019**, *9*, 257. [\[CrossRef\]](#)
10. Rodrigo-Comino, J. Five decades of soil erosion research in “terroir”: The state-of-the-art. *Earth-Sci. Rev.* **2018**, *179*, 436–447. [\[CrossRef\]](#)
11. Poni, S.; Frioni, T.; Gatti, M. Vineyard “naturalness”: Principles and challenges. *Aust. J. Grape Wine Res.* **2025**, *31*, 3247228. [\[CrossRef\]](#)
12. Rusch, A. Nature-based solutions to increase sustainability and resilience of vineyard-dominated landscapes. *Basic Appl. Ecol.* **2025**, *82*, 70–78. [\[CrossRef\]](#)
13. Kaye, J.P.; Quemada, M. Using cover crops to mitigate and adapt to climate change: A review. *Agron. Sustain. Dev.* **2017**, *37*, 4. [\[CrossRef\]](#)
14. Chalise, D.; Kumar, L.; Kristiansen, P. Land degradation by soil erosion in Nepal: A review. *Soil Syst.* **2019**, *3*, 12. [\[CrossRef\]](#)
15. O’Brien, F.; Nesbitt, A.; Sykes, R.; Kemp, B. Regenerative viticulture and climate change resilience. *OENO One* **2025**, *59*, 8089. [\[CrossRef\]](#)
16. Trenberth, K.E. Changes in precipitation with climate change. *Clim. Res.* **2011**, *47*, 123–138. [\[CrossRef\]](#)
17. Baiamonte, G.; Crescimanno, G.; Parrino, F.; De Pasquale, C. Effect of biochar on the physical and structural properties of a sandy soil. *CATENA* **2019**, *175*, 294–303. [\[CrossRef\]](#)
18. Cerdà, A.; Rodrigo-Comino, J. Regional farmers’ perception and societal issues in vineyards affected by high erosion rates. *Land* **2021**, *10*, 205. [\[CrossRef\]](#)
19. Biddoccu, M.; Ferraris, S.; Opsi, F.; Cavallo, E. Long-term monitoring of soil management effects on runoff and soil erosion in sloping vineyards in Alto Monferrato (North-West Italy). *Soil Tillage Res.* **2016**, *155*, 176–189. [\[CrossRef\]](#)
20. Tarolli, P.; Straffelini, E. Agriculture in hilly and mountainous landscapes: Threats, monitoring and sustainable management. *Geogr. Sustain.* **2020**, *1*, 70–76. [\[CrossRef\]](#)
21. Carrivick, J.L.; Smith, M.W.; Quincey, D.J. *Structure from Motion in the Geosciences*; John Wiley & Sons: Hoboken, NJ, USA, 2016. [\[CrossRef\]](#)
22. Meinen, B.U.; Robinson, D.T. Mapping erosion and deposition in an agricultural landscape: Optimization of UAV image acquisition schemes for SfM-MVS. *Remote Sens. Environ.* **2020**, *239*, 111666. [\[CrossRef\]](#)
23. Arriola-Valverde, S.; Villalobos-Avellan, L.C.; Villagra-Mendoza, K.; Rimolo-Donadio, R. Erosion quantification in runoff agriculture plots by multitemporal high resolution UAS digital photogrammetry. *IEEE J. Sel. Top. Appl. Earth Obs. Remote Sens.* **2020**, *13*, 6326–6336. [\[CrossRef\]](#)

24. Straffelini, E.; Pijl, A.; Otto, S.; Marchesini, E.; Pitacco, A.; Tarolli, P. A high-resolution physical modelling approach to assess runoff and soil erosion in vineyards under different soil managements. *Soil Tillage Res.* **2022**, *222*, 105418. [[CrossRef](#)]
25. Harwin, S.; Lucieer, A. Assessing the Accuracy of Georeferenced Point Clouds Produced via Multi-View Stereopsis from Unmanned Aerial Vehicle (UAV) Imagery. *Remote Sens.* **2012**, *4*, 1573–1599. [[CrossRef](#)]
26. Eltner, A.; Kaiser, A.; Castillo, C.; Rock, G.; Neugirg, F.; Abellán, A. Image-Based Surface Reconstruction in Geomorphometry—Merits, Limits and Developments. *Earth Surf. Dyn.* **2016**, *4*, 359–389. [[CrossRef](#)]
27. Medeiros, B.M.; Cândido, B.; Jimenez, P.A.J.; Avanzi, J.C.; Silva, M.L.N. UAV-Based Soil Water Erosion Monitoring: Current Status and Trends. *Drones* **2025**, *9*, 305. [[CrossRef](#)]
28. Nearing, M.A.; Lane, L.J.; Lopes, V.L. Modeling soil erosion. In *Soil Erosion Research Methods*; Routledge: New York, NY, USA, 1994.
29. Laflen, J.M.; Lane, L.J.; Foster, G.R. WEPP: A new generation of erosion prediction technology. *J. Soil Water Conserv.* **1991**, *46*, 34–38. [[CrossRef](#)]
30. Mitsova, H.; Thaxton, C.; Hofierka, J.; McLaughlin, R.; Moore, A.; Mitas, L. Path sampling method for modeling overland water flow, sediment transport, and short term terrain evolution in open source GIS. *Dev. Water Sci.* **2004**, *55*, 1479–1490. [[CrossRef](#)]
31. Renard, K.G.; Foster, G.R.; Weesies, G.A.; Porter, J.P. RUSLE: Revised universal soil loss equation. *J. Soil Water Conserv.* **1991**, *46*, 30–33. [[CrossRef](#)]
32. Tang, Q.; Xu, Y.; Bennett, S.J.; Li, Y. Assessment of soil erosion using RUSLE and GIS: A case study of the Yangou watershed in the Loess Plateau, China. *Environ. Earth Sci.* **2015**, *73*, 1715–1724. [[CrossRef](#)]
33. Alewell, C.; Borrelli, P.; Meusburger, K.; Panagos, P. Using the USLE: Chances, challenges and limitations of soil erosion modelling. *Int. Soil Water Conserv. Res.* **2019**, *7*, 203–225. [[CrossRef](#)]
34. Patriche, C.V. Applying RUSLE for soil erosion estimation in Romania under current and future climate scenarios. *Geoderma Reg.* **2023**, *34*, e00687. [[CrossRef](#)]
35. Chakraborty, R.; Ali, T.; Pal, T.; Pande, C.B.; Elaksher, A.F.; Abioui, M. Climate change and land use dynamics: Modeling soil erosion scenarios to achieve sustainable development goals. *Earth Syst. Environ.* **2025**, *10*, 749–774. [[CrossRef](#)]
36. Bagarello, V.; Ferro, V.; Pampaloni, V. A new version of the USLE-MM for predicting bare plot soil loss at the Sparacia (South Italy) experimental site. *Hydrol. Process.* **2015**, *29*, 4210–4219. [[CrossRef](#)]
37. Porto, P.; Bacchi, M.; Preiti, G.; Romeo, M.; Monti, M. Combining plot measurements and a calibrated RUSLE model to investigate recent changes in soil erosion in upland areas in Southern Italy. *J. Soils Sediments* **2022**, *22*, 1010–1022. [[CrossRef](#)]
38. Todisco, F.; Vergni, L.; Ortenzi, S.; Di Matteo, L. Soil Loss Estimation Coupling a Modified USLE Model with a Runoff Correction Factor Based on Rainfall and Satellite Soil Moisture Data. *Water* **2022**, *14*, 2081. [[CrossRef](#)]
39. Todisco, F.; Massimi Alunno, A.; Vergni, L. Spatial Distribution, Temporal Behaviour, and Trends of Rainfall Erosivity in Central Italy Using Coarse Data. *Water* **2025**, *17*, 801. [[CrossRef](#)]
40. Guimarães, H.; Martins, M.; Guiomar, N.; Kelly, C.; Vieira, D.; Nóvoa, T.; Brito, I.; Zoka, M.; Prats, S.; Cerdà, A.; et al. Outlook on the knowledge gaps to reduce soil erosion. *Soils Eur.* **2025**, *1*, e150281. [[CrossRef](#)]
41. ISTAT. *7° Censimento Generale dell'Agricoltura: Risultati Definitivi*; Istituto Nazionale di Statistica: Roma, Italy, 2022.
42. Zizioli, D.; Meisina, C.; Valentino, R.; Montrasio, L. Comparison between different approaches to modeling shallow landslide susceptibility: A case history in Oltrepò Pavese, Northern Italy. *Nat. Hazards Earth Syst. Sci.* **2013**, *13*, 559–573. [[CrossRef](#)]
43. Bosino, A.; Pellegrini, L.; Omran, A.; Bordoni, M.; Meisina, C.; Maerker, M. Litho-structure of the Oltrepò Pavese, Northern Apennines (Italy). *J. Maps* **2019**, *15*, 382–392. [[CrossRef](#)]
44. Bosino, A.; Szatten, D.A.; Omran, A.; Crema, S.; Crozi, M.; Becker, R.; Bettoni, M.; Schillaci, C.; Maerker, M. Assessment of suspended sediment dynamics in a small ungauged badland catchment in the Northern Apennines (Italy) using an in-situ laser diffraction method. *CATENA* **2022**, *209*, 105796. [[CrossRef](#)]
45. Gambarani, A.; Bordoni, M.; Giganti, M.; Vivaldi, V.; Gatti, M.; Poni, S.; Vercesi, A.; Meisina, C. Multi-year assessment of soil moisture dynamics under nature-based vineyard floor management in the Oltrepò Pavese (Northern Italy). *Agriculture* **2026**, *16*, 316. [[CrossRef](#)]
46. Cunial, L.; Diti, I.; Bonini, P.; Patelli, R.; Gatti, M.; Cola, G.; Bordoni, M.; Nguyen, T.N.A.; Meisina, C.; Confalonieri, R.; et al. Novel termination techniques of winter cover crops in the vineyard: Effects on physiology and performance of Pinot Noir and Malvasia di Candia aromatica grapevines. *Eur. J. Agron.* **2025**, *164*, 127514. [[CrossRef](#)]
47. Scoccimarro, E.; Bellucci, A.; Peano, D. *CMCC CMCC-CM2-VHR4 Model Output Prepared for CMIP6 HighResMIP*, Version 20220627; Earth System Grid Federation: Livermore, CA, USA, 2017. [[CrossRef](#)]
48. von Storch, J.-S.; Putrasahan, D.; Lohmann, K.; Gutjahr, O.; Jungclaus, J.; Bittner, M.; Haak, H.; Wieners, K.; Giorgetta, M.; Reick, C.; et al. *MPI-M MPI-ESM1.2-XR Model Output Prepared for CMIP6 HighResMIP*, Version 20220616; Earth System Grid Federation: Livermore, CA, USA, 2017. [[CrossRef](#)]
49. EC-Earth Consortium (EC-Earth). *EC-Earth3P-HR Model Output Prepared for CMIP6 HighResMIP*, Version 20220602; Earth System Grid Federation: Livermore, CA, USA, 2018. [[CrossRef](#)]
50. Sen, Z. Innovative trend analysis methodology. *J. Hydrol. Eng.* **2012**, *17*, 1042–1046. [[CrossRef](#)]

51. Wischmeier, W.H.; Smith, D.D. *Predicting Rainfall Erosion Losses: A Guide to Conservation Planning*; USDA Agricultural Handbook No. 537; USDA: Beltsville, MD, USA, 1978.
52. Richardson, C.W.; Foster, G.R.; Wright, D.A. Estimation of erosion index from daily rainfall amount. *Trans. ASAE* **1983**, *26*, 153–156. [[CrossRef](#)]
53. Bagarello, V.; Ferro, V. *Erosione e Conservazione del Suolo*; McGraw-Hill: Columbus, OH, USA, 2006; Volume 1, pp. 1–539.
54. Wischmeier, W.H.; Johnson, C.B.; Cross, B.V. A soil erodibility nomograph for farmland and construction sites. *J. Soil Water Conserv.* **1971**, *26*, 189–193.
55. Zangar, C.N. *Theory and Problems of Water Percolation*; U.S. Bureau of Reclamation, Engineering Monograph No. 8; U.S. Bureau of Reclamation: Denver, CO, USA, 1953.
56. Moore, I.D.; Burch, G.J. Physical basis of the length-slope factor in the Universal Soil Loss Equation. *Soil Sci. Soc. Am. J.* **1986**, *50*, 1294–1298. [[CrossRef](#)]
57. Moore, I.D.; Wilson, J.P. Length-slope factors for the Revised Universal Soil Loss Equation: Simplified method of estimation. *J. Soil Water Conserv.* **1992**, *47*, 423–428. [[CrossRef](#)]
58. Yang, X.; Tang, G.; Xiao, C.; Gao, Y.; Zhu, S. The scaling method of specific catchment area from DEMs. *J. Geogr. Sci.* **2011**, *21*, 689–704. [[CrossRef](#)]
59. Paroissien, J.-B.; Lagacherie, P.; Le Bissonnais, Y. A regional-scale study of multi-decennial erosion of vineyard fields using vine-stock unearthing–burying measurements. *CATENA* **2010**, *82*, 159–168. [[CrossRef](#)]
60. Prosdocimi, M.; Cerdà, A.; Tarolli, P. Soil water erosion on Mediterranean vineyards: A review. *CATENA* **2016**, *141*, 1–21. [[CrossRef](#)]
61. Novara, A.; Catania, V.; Tolone, M.; Gristina, L.; Laudicina, V.A.; Quatrini, P. Cover crop impact on soil organic carbon, nitrogen dynamics and microbial diversity in a Mediterranean semi-arid vineyard. *Sustainability* **2020**, *12*, 3256. [[CrossRef](#)]
62. Brenot, J.; Quiquerez, A.; Petit, C.; Garcia, J.-P. Erosion rates and sediment budgets in vineyards at 1-m resolution based on stock unearthing (Burgundy, France). *Geomorphology* **2008**, *100*, 345–355. [[CrossRef](#)]
63. Rodrigo-Comino, J.; Cerdà, A. Improving stock unearthing method to measure soil erosion rates in vineyards. *Ecol. Indic.* **2018**, *85*, 509–517. [[CrossRef](#)]
64. MacFarland, T.W. *Two-Way Analysis of Variance*; Springer: New York, NY, USA, 2012.
65. Azimi Sardari, M.R.; Bazrafshan, O.; Panagopoulos, T.; Sardooi, E.R. Modeling the impact of climate change and land use change scenarios on soil erosion at the Minab Dam Watershed. *Sustainability* **2019**, *11*, 3353. [[CrossRef](#)]
66. Panagos, P.; Ballabio, C.; Himics, M.; Scarpa, S.; Matthews, F.; Bogonos, M.; Poesen, J.; Borrelli, P. Projections of soil loss by water erosion in Europe by 2050. *Environ. Sci. Policy* **2021**, *124*, 380–392. [[CrossRef](#)]
67. Fatima, B.; Rachid, H.; Abdeldjalil, B.; Abdessalam, O.; Mohamed, B.; Alfagham, A.T.; Tariq, A. Monitoring and forecasting water erosion in response to climate change effects using the integration of the global RUSLE/SDR model and predictive models. *Appl. Soil Ecol.* **2025**, *206*, 105910. [[CrossRef](#)]
68. Borrelli, P.; Robinson, D.A.; Panagos, P.; Lugato, E.; Yang, J.E.; Alewell, C.; Wuepper, D.; Montanarella, L.; Ballabio, C. Land use and climate change impacts on global soil erosion by water (2015–2070). *Proc. Natl. Acad. Sci. USA* **2020**, *117*, 21994–22001. [[CrossRef](#)] [[PubMed](#)]
69. Dash, S.S.; Maity, R. Effect of climate change on soil erosion indicates a dominance of rainfall over LULC changes. *J. Hydrol. Reg. Stud.* **2023**, *47*, 101373. [[CrossRef](#)]
70. Du, C.; Bai, X.; Li, Y.; Tan, Q.; Zhao, C.; Luo, G.; Wang, J.; Wu, L.; Li, C.; Li, J.; et al. The restoration of karst rocky desertification has enhanced the carbon sequestration capacity of the ecosystem in southern China. *Glob. Planet. Change* **2024**, *243*, 104602. [[CrossRef](#)]
71. Verheijen, F.G.A.; Jones, R.J.A.; Rickson, R.J.; Smith, C.J. Tolerable versus actual soil erosion rates in Europe. *Earth-Sci. Rev.* **2009**, *94*, 23–38. [[CrossRef](#)]
72. Trabucchi, M.; Puente, C.; Comin, F.A.; Olague, G.; Smith, S.V. Mapping erosion risk at the basin scale in a Mediterranean environment with opencast coal mines to target restoration actions. *Reg. Environ. Change* **2012**, *12*, 675–687. [[CrossRef](#)]
73. Farhan, Y.; Nawaiseh, S. Spatial assessment of soil erosion risk using RUSLE and GIS techniques. *Environ. Earth Sci.* **2015**, *74*, 4649–4669. [[CrossRef](#)]
74. Borrelli, P.; Panagos, P.; Alewell, C.; Ballabio, C.; de Oliveira Fagundes, H.; Haregeweyn, N.; Lugato, E.; Maerker, M.; Poesen, J.; Vanmaercke, M.; et al. Policy implications of multiple concurrent soil erosion processes in European farmland. *Nat. Sustain.* **2023**, *6*, 103–112. [[CrossRef](#)]
75. Di Stefano, C.; Nicosia, A.; Pampalona, V.; Ferro, V. Soil loss tolerance in the context of the European Green Deal. *Heliyon* **2023**, *9*, e12869. [[CrossRef](#)]
76. Martínez-Casasnovas, J.A.; Ramos, M.C.; García-Hernández, D. Effects of land-use changes in vegetation cover and sidewall erosion in a gully head of the Penedès region (northeast Spain). *Earth Surf. Process. Landf.* **2009**, *34*, 1927–1937. [[CrossRef](#)]

77. Rodrigo-Comino, J.; Iserloh, T.; Morvan, X.; Malam Issa, O.; Naisse, C.; Keesstra, S.D.; Cerdà, A.; Prosdocimi, M.; Arnáez, J.; Lasanta, T.; et al. Soil erosion processes in European vineyards: A qualitative comparison of rainfall simulation measurements in Germany, Spain and France. *Hydrology* **2016**, *3*, 6. [[CrossRef](#)]
78. Maqbool, S.; Hassan, M.A.; Xia, X.; York, L.M.; Rasheed, A.; He, Z. Root system architecture in cereals: Progress, challenges and perspective. *Plant J.* **2022**, *110*, 23–42. [[CrossRef](#)]
79. Gonzalez-Rizzo, S.; Laporte, P.; Crespi, M.; Frugier, F. Legume root architecture: A peculiar root system. In *Root Development*; Beeckman, T., Ed.; Wiley: Hoboken, NJ, USA, 2009; Chapter 10. [[CrossRef](#)]
80. Andrenelli, M.C.; Pellegrini, S.; Fila, G.; Becagli, C.; Valboa, G.; Vignozzi, N. Erosion assessment by a fast and low-cost procedure in a vineyard under different soil management. *Agriculture* **2025**, *15*, 2218. [[CrossRef](#)]
81. Wang, Y.; Yu, A.; Shang, Y.; Wang, P.; Wang, F.; Yin, B.; Liu, Y.; Zhang, D.; Chai, Q. Research progress on the improvement of farmland soil quality by green manure. *Agriculture* **2025**, *15*, 768. [[CrossRef](#)]
82. Bagagiolo, G.; Biddoccu, M.; Rabino, D.; Cavallo, E. Effects of rows arrangement, soil management, and rainfall characteristics on water and soil losses in Italian sloping vineyards. *Environ. Res.* **2018**, *166*, 690–704. [[CrossRef](#)] [[PubMed](#)]
83. Granata, F.; Zhu, S.; Di Nunno, F. Hydrological extremes in the Mediterranean basin: Interactions, impacts, and adaptation in the face of climate change. *Reg. Environ. Change* **2025**, *25*, 100. [[CrossRef](#)]
84. Treppiedi, D.; Francipane, A.; Noto, L.V. Projecting Depth-Duration-Frequency Curves for Future Climate: A Case Study in the Mediterranean Area. *Water Resour. Manag.* **2025**, *39*, 4409–4427. [[CrossRef](#)]
85. Piccarreta, M.; Bentivenga, M.; Piccarreta, R. Trend analysis of hourly rainfall in the Mediterranean: A case study of the Basilicata Region, Southern Italy (2001–2024). *Theor. Appl. Climatol.* **2026**, *157*, 10. [[CrossRef](#)]
86. Darouich, H.; Ramos, T.B.; Pereira, L.S.; Rabino, D.; Bagagiolo, G.; Capello, G.; Simionesei, L.; Cavallo, E.; Biddoccu, M. Water use and soil water balance of Mediterranean vineyards under rainfed and drip irrigation management: Evapotranspiration partition and soil management modelling for resource conservation. *Water* **2022**, *14*, 554. [[CrossRef](#)]
87. Fressard, M.; Cossart, E.; Chaize, B. Pluri-decennial erosion rates using SUM/ISUM and sediment traps survey in the Mercurey vineyards (Burgundy, France). *Geomorphology* **2022**, *403*, 108181. [[CrossRef](#)]
88. Andualet, T.G.; Hewa, G.A.; Myers, B.R.; Peters, S.; Boland, J. Erosion and sediment transport modeling: A systematic review. *Land* **2023**, *12*, 1396. [[CrossRef](#)]

Disclaimer/Publisher’s Note: The statements, opinions and data contained in all publications are solely those of the individual author(s) and contributor(s) and not of MDPI and/or the editor(s). MDPI and/or the editor(s) disclaim responsibility for any injury to people or property resulting from any ideas, methods, instructions or products referred to in the content.